Passive Electrostatic Recycling Spectrometer of Desk-Top Size for Charged Particles of Low Kinetic Energy

D. R. Tessier,[1] Y. Niu,[1] D. P. Seccombe,[1] T. J. Reddish,[1,*] A. J. Alderman,[2] B. G. Birdsey,[2] F. H. Read,[3] and P. Hammond[2,†]

[1]*Department of Physics, University of Windsor, Windsor, Ontario N9B 3P4, Canada*

[2]*CAMSP, School of Physics, University of Western Australia, Crawley WA 6009, Australia*

[3]*School of Physics and Astronomy, University of Manchester, Manchester M13 9PL, United Kingdom*

(Received 14 August 2007; published 18 December 2007)

A passive electrostatic recycling spectrometer for charged particles is described and demonstrated to store electrons with typical kinetic energies of tens of eV. The design of the charged particle optics and the basic operating characteristics of the storage ring are discussed. The storage lifetime achieved is $\sim 50\ \mu$s, which is target gas pressure limited and corresponds to ~ 200 orbits of the 0.65 m orbital circumference. The storage ring also has controllable energy dispersive elements enabling it to operate as a spectroscopic device.

DOI: 10.1103/PhysRevLett.99.253201 PACS numbers: 39.10.+j, 29.20.Dh, 34.85.+x, 41.75.-i

There has been sustained interest in the manipulation and control of electrons, and other charged particles since the pioneering days of J. J. Thomson. New areas of physics have emerged over the last century that rely on such knowledge, resulting in a myriad of applications from semiconductor devices to particle accelerators. Particle trapping techniques, for example, whether for atoms, ions, or polarized molecules continue to revolutionize certain classes of experiments and enable studies hitherto impossible. In the relativistic regime, synchrotrons, betatrons and other cyclic accelerators confine charged particles using magnetic fields and rf electric fields.

A typical ''crossed beam'' experiment in atomic and molecular physics consists of a controlled beam of electrons, positrons, or ions that collides orthogonally with a gas beam. In general, a substantial amount of effort is put into optimizing the current, energy variability, energy resolution and spatial definition of the projectile beam. In such beams particles are given only one opportunity of interacting with the gaseous target and are then discarded. This is inefficient because the vast majority of the charged particles do not interact with the target gas due to the small collisional cross sections. In some applications this is severely limiting, as the particle source flux can be inherently low (e.g., [1–3]) or challenging to generate.

Here we introduce an innovative electrostatic apparatus for the storage of low energy charged particles (<150 eV) orbiting in a desktop sized ring with a view to enabling a new class of high precision measurements. For the present apparatus, called an electron recycling spectrometer (ERS) and shown schematically in Fig. 1, the experiments described here explore only the storage capability and characteristics of the racetrack shaped ring coupled with a simple external pulsed electron source. Imagine a spherical capacitor; electrons of appropriate energies and suitable (r, θ, φ) values undergo Kepler orbits indefinitely in the $1/r^2$ electric field between the two spherical electrodes. The ERS makes this ''thought experiment'' practicable by splitting the capacitor in half, separating the two hemispheres, and filling the intervening space with electrostatic lenses. Electrons unscattered in the target gas beam are collected and returned for multiple crossings through the gas beam. This ''recycling'' concept is analogous to a trap; albeit the charged particles here are confined in stable spatial orbits where the underlying stability conditions of storage rings are still applicable [4]. Unlike most storage rings, the ERS is ''passive''; it has no active feedback components. The ERS has a circumference of 0.65 m, typical orbit times of ~ 300 ns, and can operate up to $\sim 1 \times 10^{-5}$ Torr while still recycling spatially and temporally well-defined electron bunches of controllable energy.

The system can be adapted in a variety of ways for use with positrons, polarized electrons and ions. For example, a pulse of positrons from an external accumulator could be recycled around the ring during the next period of charge buildup in the accumulator. An alternate configuration

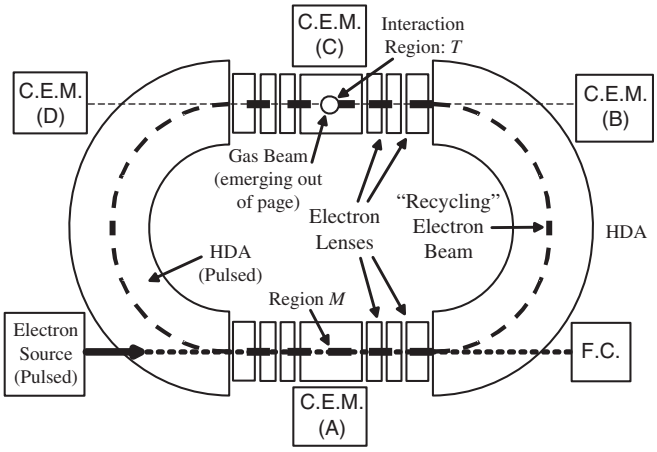

FIG. 1. Schematic of the electrostatic charged particle recycling system for electrons. Particle detection is achieved via channel electron multiplier's located in key positions around the spectrometer.

would place the charged particle source, such as a laser photoionization electron source, internal to the ring to allow accumulation of photoelectrons of well-defined kinetic energy. If on average each photoelectron makes N orbits of the ring, then a photoelectron source generating a flux a factor N less than a single pass apparatus would yield the same overall photoelectron flux, but with an improved energy resolution, due to the reduced source photoion space charge of a less intense source [2].

Over the last decade electrostatic storage rings for nonrelativistic ion beams have been developed for use in atomic and molecular physics [5–10]. These devices typically have circumferences of 7–35 m, operating energies of ~20–50 keV with vacuum base pressures of 10^{-11}–10^{-13} Torr. They are complimented by the compact ''fast'' ion trap developed by Zajfman and co-workers [11,12]. The ERS has features analogous to both electrostatic ion storage rings and Zajfman's linear ion beam ''resonator.'' The change of mass scale from ions to electrons is very significant because of the much shorter orbital time scales. The ERS allows, for the first time, the orbital confinement of low energy electrons.

In the ERS (Fig. 1), electrons emitted from a hot tungsten filament are collimated into a beam in a short electron gun. This beam is injected in a pulse ~50 ns wide through an aperture in the outer hemisphere of a hemispherical deflector analyzer (HDA) in which, for the duration of the pulse, the inner and outer hemisphere voltages are temporarily set to the voltage equivalent of the pass energy, E_L, of the deflector. Following the electron injection pulse the hemisphere voltages are set to normal operating voltages, a process which takes tens of nanoseconds to reach stable, quiescent voltage levels. The injected electron bunch is transported by a four element cylinder lens (FECL) into region M (electron energy E_M), viewed by a channel electron multiplier (CEM) labeled A (see Fig. 1). A subsequent FECL transports the electron bunch from region M onto the entrance of a second HDA operating with pass energy E_U. Electrons passed by this analyzer are then focused by another FECL into region T, where electrons of energy E_T are crossed with an effusive gas target beam. This interaction region is viewed by two CEM's, C in Fig. 1, and E placed inline with the gas beam (not shown in Fig. 1). Unscattered electrons are refocused by a fourth FECL to reenter the first HDA now operating in the normal voltage regime and passing electrons of energy E_L. Electrons exiting this HDA, having completed an orbit of the ERS, then retrace similar orbital paths. In this way the electrons are recycled.

The ERS is housed in an ultrahigh vacuum chamber with a typical base pressure of 5×10^{-8} Torr. The chamber is internally double lined with mu metal and externally surrounded by orthogonal pairs of Helmholtz coils to magnetically shield the ERS to <2 mG.

Passive recycling performance is critically dependent upon minimizing mechanisms for electron loss from the recycling low energy beam. These loss mechanisms can be divided into two categories: (i) those that can be addressed by careful design and (ii) those that are inherent. Precision mechanical construction and alignment was ensured, together with the minimization of magnetic fields and electrode voltage instabilities. Oxygen-free copper ERS components were all gold plated to reduce localized surface property variations that could give rise to time varying distortions in electric fields [13]. Note that, in comparison to ion storage rings, fluctuations in electric (and magnetic) fields are particularly damaging to the passive recycling of electrons or positrons due to their much smaller mass. Inevitable loss mechanisms, namely, electron optical aberrations and collisions with residual background gas, are controlled through detailed electron optical design and suitable choice of operating pressure, respectively. Other losses, such as radiation and space charge limitations can be shown to be negligible in this case.

The design of the charged particle optics has been partly achieved using a formal matrix representation of the idealized lenses and HDA's. The general condition for stable orbits is given by:

$$\tfrac{1}{2}|\mathrm{Tr}(M_{\mathrm{ss}})| \leq 1, \tag{1}$$

where M_{ss} is the overall transfer matrix for one complete orbit [4]. While there can be no overall acceleration in one orbit, one can achieve the stability condition in a variety of ways, so it is not necessary to have $E_L = E_U$ or $E_T = E_M$ [14]. Consequently, the racetrack configuration of Fig. 1 is more like a roller coaster in electron energy. Since HDA's are energy dispersive, only electrons within a specific energy range, ΔE_{ERS}, will be recycled. Utilizing the well-known properties of HDA's enables useful flexibility in the ERS operation. (i) When $E_U \ll E_L$, ΔE_{ERS} is largely determined by E_U and the HDA with E_L acts more like a mirror than a prism. Moreover, if ΔE_{ERS} is less than the inherent energy spread from the electron gun, ΔE_S, (as in this study), then the ERS also acts as an energy filter. (ii) Alternatively, if $\Delta E_S \ll \Delta E_{\mathrm{ERS}}$, then both HDA's act like mirrors. This latter mode, for instance, would allow the preservation and optimisation of the energy profile of ultrahigh energy resolved electron beams from laser photoionization sources [2,3].

Charged particle trajectory integrations, which compliment the matrix approach and include the role of lens and HDA aberrations, were performed using CPO-3D [15]. Both approaches were used in parallel to predict the initial voltage set for the ERS electrodes.

Achieving recycling in practice is a delicate tuning process requiring the use of the Faraday Cup (FC) and the four electron monitors shown in Fig. 1 in combination with switching the HDA's between recycling and nonrecycling modes. Once the ERS is tuned, the measured lens voltages compare favorably with those predicted by the analytical models.

Data demonstrating storage of electrons in the ERS following electron injection are shown in Fig. 2. This timing spectrum was obtained with CEM (C), orthogonal

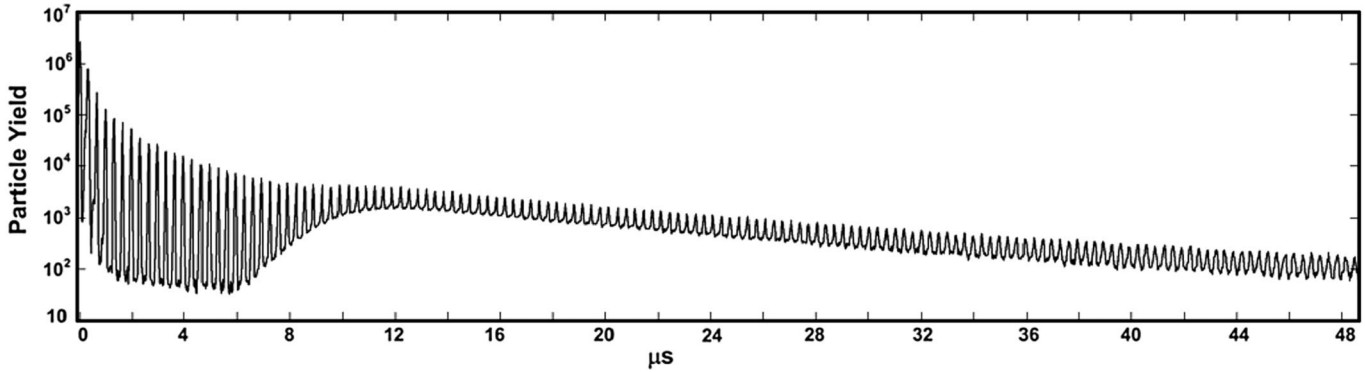

FIG. 2. A logarithmic plot of the signal yield in CEM (C) from 30 eV (E_T) electron collisions with helium at a chamber pressure of 7×10^{-7} Torr as a function of time after the initial electron injection. The spectrum shows ~150 sharp peaks due to scattered electrons whose time structure corresponds to that of the recycling electron beam and a broad underlying continuum due to metastable helium atoms.

to both the electron and gas beams, with $E_L = 18$ eV and $E_U = 4$ eV. The recorded signal consists of two components, one arising from 30 eV electrons elastically scattered from helium at 90° and a second from excited helium atoms in metastable states [2,16]. Electrons appear as repetitive peaks spaced at 330 ns intervals corresponding to sequential orbits of the electrons stored in the ERS. The metastable atom signal is broad in time, with an onset at ~6 μs after electron injection, and underlies the sharp electron peaks. The delayed onset corresponds to the time-of-flight of thermal atoms with their velocity spread causing atoms excited by sequential orbits of the electron bunch to have overlapping times of flight. Analysis of the spectrum in Fig. 2 reveals that after ~15 μs the electron peak heights have an exponential decay characterized by $\tau_H \approx 13.6$ μs. However, the area within each peak is a better comparative measure and its decay rate is slower with $\tau_A \approx 19.4$ μs.

The spectrum in Fig. 2 shows that electrons recycling in the ERS performed over 150 orbits traveling ~100 m in a chamber pressure of 7×10^{-7} Torr. The full-width half maximum (FWHM) bunch width variation as a function of orbit number is shown in Fig. 3. The bunch width reduces from 51 to 45 ns in the first few orbits because $\Delta E_S > \Delta E_{\mathrm{ERS}}$ and consequently the HDA's and apertures eliminate trajectories with inappropriate energy, radial distance and angle for sustained recycling. After the first $\approx$5 orbits, the bunch width increases with orbit number. In the linear electrostatic ion trap, Pedersen *et al.* [17] observe very similar behavior despite the differences in physical geometry and the ~1000 factor in time scale. They show the recycling pulse width, W_n, increases with orbit number n as

$$W_n = \sqrt{W_0^2 + n^2 \Delta T^2}, \tag{2}$$

where W_0 is the initial temporal width. For the ERS, W_0 is largely determined by the duration of the electron injection pulse. The time spread per orbit, ΔT, consists of two components: (i) ΔT_{ERS}, the time spread within the ERS for an electron of given energy due to the possible ranges of positions and angles, (r, θ), giving rise to a range of orbit times. These different trajectories depend on the geometrical configuration and operating potentials of the ERS; (ii) ΔT_S is due to the inherent spread in the electron energies at $t = 0$ and is usually solely a property of the source. In the present experiment, where $\Delta E_S > \Delta E_{\mathrm{ERS}}$, we define this "initial" time spread as that after the post-injection "clean up" of the first ~5 orbits. Taking ΔT_{ERS} and ΔT_S to be independent, the total time spread for each orbit bunch in the ERS is given by

$$\Delta T^2 = \Delta T_{\mathrm{ERS}}^2 + \Delta T_S^2. \tag{3}$$

This assumes no coupling between these processes from internal mechanisms within the beam, such as Coulomb interactions (space charge effects), or from external perturbers, such as residual gas scattering and electrical noise on the electrodes. Under these conditions, ΔT will remain a constant for all orbits as each electron moves independently of the others, preserving its initial orbital period. There is clearly excellent agreement with the form of Eq. (2) with least squares fit values of $W_0 = 46.5 \pm 0.1$ ns and $\Delta T = 0.74 \pm 0.05$ ns (see solid line, Fig. 3).

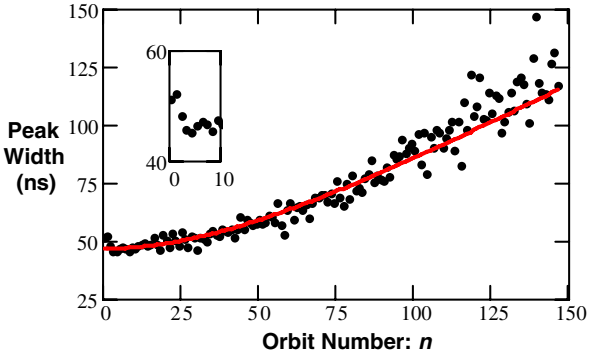

FIG. 3 (color online). Time width of the stored electron bunch as a function of orbit number n for the peaks in Fig. 2. The solid line is a fit to Eq. (2), as discussed in the text.

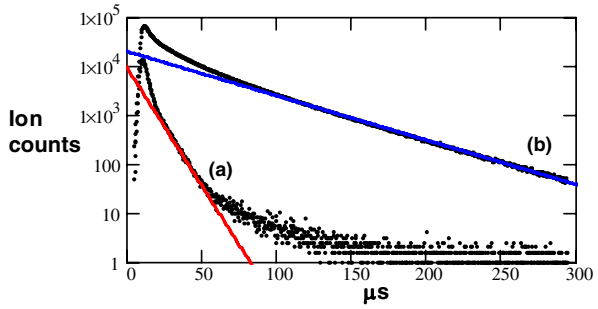

FIG. 4 (color online). Helium ion "time-of-flight" distributions at CEM (E) for (a) nonrecycling and (b) recycling modes. The asymptotic linear decay rates are (a) $\tau_{NR} \approx 9$ μs and (b) $\tau_{NR} \approx 48$ μs; see text for discussion.

Consequently, the underlying assumptions of this diffusion process describe the electron dynamics of the ERS under the present operating conditions.

Long term storage within the ERS has been investigated by measuring helium ion time-of-flight (TOF) distributions with CEM (E), situated opposite the effusive gas beam. A typical spectrum of the He^+ yield as a function of time after the electron injection pulse over a 300 μs time window is shown in Fig. 4 for a chamber gas pressure of 5×10^{-7} Torr. The ion distribution in the nonrecycling mode was also recorded for the same data acquisition time and is also displayed in Fig. 4. For these spectra, $E_L = E_U = 18$ eV and the orbit time was 240 ns [measured at CEM (A)]. The nonrecycling mode is achieved by pulsing the electron gun in an identical manner to the recycling mode, but with the HDA voltages not being switched after electron injection making it physically impossible to recycle. In this mode, the observed signal corresponds to the inherent time of flight for helium ions created with a ~50 ns pulse of electrons. The peak in the ion distribution occurs at ≈13 μs after the electron pulse and the distribution has a characteristic decay time of $\tau_{NR} \approx 9$ μs. The ion distribution in the recycling mode has a longer decay time $\tau_R \approx 48$ μs, although there is measurable ion yield at ~7 times that value. Very few ions are detected after 60 and 340 μs in the nonrecycling and recycling modes, respectively. Consequently, ions detected at $t = 340$ μs originate from

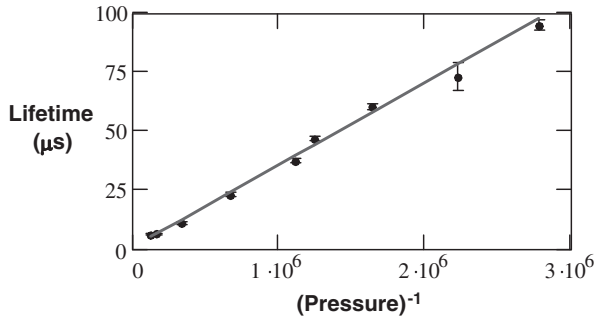

FIG. 5. Decay lifetimes, τ_R, obtained from the asymptotic linear decay rates in helium (see Fig. 4) for a range of chamber gas pressures, P, spanning from 3.6×10^{-7} to 8.0×10^{-6} Torr.

stored electrons in the ERS between $t = 280$ and 327 μs. We conclude that at this operating pressure some electrons in the injected bunch were stored for ~5 lifetimes, equivalent to ~1000 orbits, corresponding to an electron of mean energy ~20 eV traveling over 650 m.

Helium ion TOF spectra were measured as a function of gas pressure, P, for identical ERS tuning and pulsing conditions with $E_L = E_U = 15$ eV and $E_T = 40$ eV. The characteristic decay time, τ_R, determined at each pressure are displayed in Fig. 5, plotted against $1/P$ and show a clear linear relationship. This demonstrates that the dominant loss mechanism is due to collisions with the target gas, as mean free path, $\lambda \propto 1/P$ and $\tau_R \propto \lambda$.

This experimental study shows the ERS to be sufficiently stable to the potential loss mechanisms and to have enough stored current to perform gas phase collision experiments that are target pressure limited. Measurements are currently underway to quantify the stored current and determine the energy resolution of the recycling beam as a function of storage time, in order to compare it with theory [14]. The ability to scan E_T to perform energy and time dependent studies will also be explored.

The authors wish to acknowledge John Corner and Alan Bott (University of Newcastle upon Tyne, UK) for precision engineering. Financial support for this work was provided by the Paul Instrument Fund (UK); ARC (Australia); CFI, OIT, NSERC, and the University of Windsor (Canada).

*reddish@uwindsor.ca
†phammond@physics.uwa.edu.au

[1] S. J. Gilbert *et al.*, Nucl. Instrum. Methods Phys. Res., Sect. B **171**, 81 (2000).
[2] A. Gopalan *et al.*, Eur. Phys. J. D **22**, 17 (2003).
[3] J. Bömmels *et al.*, Phys. Rev. A **71**, 012704 (2005).
[4] E. D. Courant and H. S. Snyder, Ann. Phys. (Leipzig) **3**, 1 (1958).
[5] S. P. Møller, Nucl. Instrum. Methods Phys. Res., Sect. A **394**, 281 (1997).
[6] S. P. Møller and U. V. Pedersen, Phys. Scr. **T92**, 105 (2001).
[7] T. Tanabe *et al.*, Nucl. Instrum. Methods Phys. Res., Sect. A **482**, 595 (2002).
[8] C. P. Welsch *et al.*, Phys. Rev. ST Accel. Beams **7**, 080101 (2004).
[9] S. Jinnoa *et al.*, Nucl. Instrum. Methods Phys. Res., Sect. A **572**, 568 (2007).
[10] L. H. Andersen, O. Heber, and D. Zajfman, J. Phys. B **37**, R57 (2004).
[11] H. B. Pedersen *et al.*, Phys. Rev. Lett. **87**, 055001 (2001).
[12] D. Zajfman *et al.*, Nucl. Instrum. Methods Phys. Res., Sect. A **532**, 196 (2004).
[13] G. Langner, J. Vac. Sci. Technol. B **8**, 1711 (1990).
[14] P. Hammond *et al.* (to be published).
[15] CPO Programs: http://www.electronoptics.com/.
[16] S. J. Buckman *et al.*, J. Phys. B **16**, 4039 (1983).
[17] H. B. Pedersen *et al.*, Phys. Rev. A **65**, 042704 (2002).